Superelastic Electron Scattering within a Magnetic Angle Changer: Determination of the Angular Momentum Transferred during Electron Excitation over All Scattering Angles

Martyn Hussey,[1] Andrew Murray,[1] William MacGillivray,[1,2] and George C. King[1]
[1]School of Physics and Astronomy, University of Manchester, Manchester, United Kingdom
[2]Southern Cross University, Lismore, New South Wales 2480, Australia
(Received 1 June 2007; published 28 September 2007)

By utilizing superelastic electron scattering from laser-excited atoms within a new magnetic angle changing device, the differential cross sections for excitation of atoms by electron impact over the complete scattering geometry are determined for the first time. In the experiments described here, these techniques are combined to reveal the angular momentum transferred to calcium atoms during electron excitation to the 4^1P_1 state, from near 0° to beyond 180°. The experiments are discussed, and results presented for energies of 45 and 55 eV. These results are compared to calculations using a distorted wave Born approximation.

DOI: 10.1103/PhysRevLett.99.133202 PACS numbers: 34.80.Dp

The detailed study of electron collision processes has a long history in the field of experimental atomic and molecular physics, with excitation [1] and ionization [2] of the target providing stringent tests of the most sophisticated theories. These comparisons are most exact when the momenta and character of the incident and scattered particles are determined in coincidence, since the full differential cross section can then be ascertained.

Although a very powerful technique for determination of cross sections, coincidence methods suffer from low detection efficiencies. This is because they are, by their nature, highly selective in the energy and momentum of the process under study. For excitation studies, the scattered electron is detected at a given angle and is time-correlated with a photon emitted from the excited target. The momentum of the incident electron ($\mathbf{k}_{\text{in}}$) and the scattered electron ($\mathbf{k}_{\text{out}}$) then define a scattering plane. The polarization of the correlated photon is determined, so that a complete description of the radiated light is ascertained. The coincidence technique therefore effectively selects a small subset of all possible scattering events, allowing accurate comparison to theory. Parameters which characterize the ''shape'' of the excited target are then calculated usually in the Natural frame [1], which has a quantization axis orthogonal to the scattering plane.

For excitation to a P state, the parameters are the angular momentum $L_\perp$ transferred to the charge cloud during the interaction, the angle γ of the charge cloud with respect to the incident electron direction, and P_{lin} which defines the ''length'' to ''width'' ratio of the charge cloud. If spin flip occurs during excitation, a parameter ρ_{00}^A is also defined which relates to the relative ''height'' of the charge cloud above the scattering plane at the origin.

Electron-photon coincidence techniques are slow since the atom that scatters the detected electron may not radiate to the photon detector, in which case no event registers. An alternative method that provides equivalent information is the superelastic scattering experiment, which adopts time reversal of the scattering event. In this technique (Fig. 1), the atom is initially excited using laser radiation directed orthogonal to the scattering plane, whose polarization is well defined (1). The incident electrons are directed in the opposite direction to those detected in a coincidence experiment (2), while the electron detector is located where the source would be. The detector measures superelastically scattered electrons that have equal energy to the incident electrons in the coincidence experiment (3).

The signal counting rates from superelastic scattering experiments are many times greater than those for coincidence experiments. This is because the laser photons are directed in a single, well-defined direction. Data are accumulated by counting the rate of superelastically scattered electrons as a function of the laser polarization. It is necessary to carefully consider the absorption, stimulated, and spontaneous emission effects of the laser radiation on

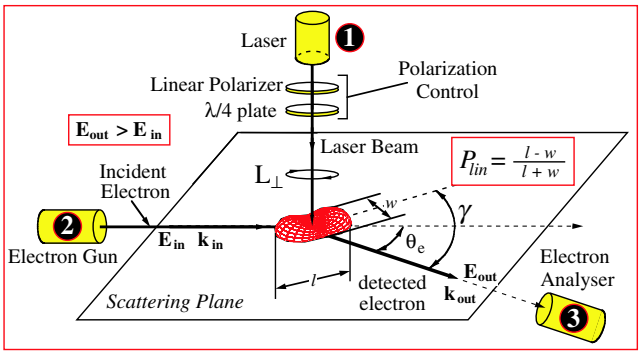

FIG. 1 (color online). The superelastic scattering geometry, which is the time-inverse of the electron-photon coincidence technique. Electrons of momentum $\mathbf{k}_{\text{in}}$ are directed at atoms prepared in an excited state by resonant laser radiation. Scattered electrons are detected with momentum $\mathbf{k}_{\text{out}}$ as a function of the scattering angle θ_e, so as to determine the natural frame parameters $L_\perp$, γ, P_{lin}.

 © 2007 The American Physical Society

the excited atoms to ensure that the natural frame parameters are correctly determined; however, these effects can be modeled accurately [3]. The angular momentum parameter $L_\perp$ is derived from the ratio of superelastically scattered electrons produced by changing the handedness of circularly polarized laser radiation, whereas γ and P_{lin} are determined using linear radiation.

In this letter, a new type of superelastic scattering process is discussed which uses a novel technique to steer electrons to and from the interaction region. This gives access to the backward scattering hemisphere for the first time for these differential cross section measurements. This magnetic angle changing (MAC) device was invented in Manchester [4], and uses well-controlled magnetic fields generated by precisely machined solenoids surrounding the interaction region. By careful design of the solenoids, two important criteria are met. The first is that the magnetic field falls off rapidly with distance so that the resulting field in the electron gun and analyzer is negligible, ensuring electrons in these components are not disturbed. The second is that electrons directed radially towards the interaction region pass through the interaction region situated at the center of the solenoids, with the additional condition that they undergo an angular deflection.

The MAC device hence acts to steer electrons into and out of the interaction region so that their angles are changed, as shown in Fig. 2. In this example, the incident electron beam has an energy of 45 eV, and the current through the solenoids sets the magnetic field to 2.5 mT at the interaction region. The MAC device is seen to steer the electrons into the interaction region so that the incident beam exits at an angle ~55° from the initial beam direction. By contrast, electrons that superelastically backscatter from the reaction ($\theta_e = 180°$) are steered to an angle ~130°, where an electron analyzer can be located. The MAC therefore allows data to be collected over scattering angles which are impossible to access using conventional electron spectrometers.

Figure 3 shows a representation of the spectrometer constructed for these studies. The atomic beam is produced by a well-collimated oven so that the Doppler profile presented to the laser beam is narrow [5]. The electron gun is located next to the oven, and the electron analyzer [6] rotates around the scattering plane on a turntable driven by a rotary feedthrough, so as to access different angles. The MAC solenoids surround the interaction region as shown. Without the MAC device operating the angular range of the analyzer is from near 0° to 145°, whereas application of the MAC device extends this to greater than 180°. The exciting laser enters the vacuum chamber through a window in the top flange, and is accurately directed through the interaction region by following a tracer diode laser beam emitted from inside the chamber.

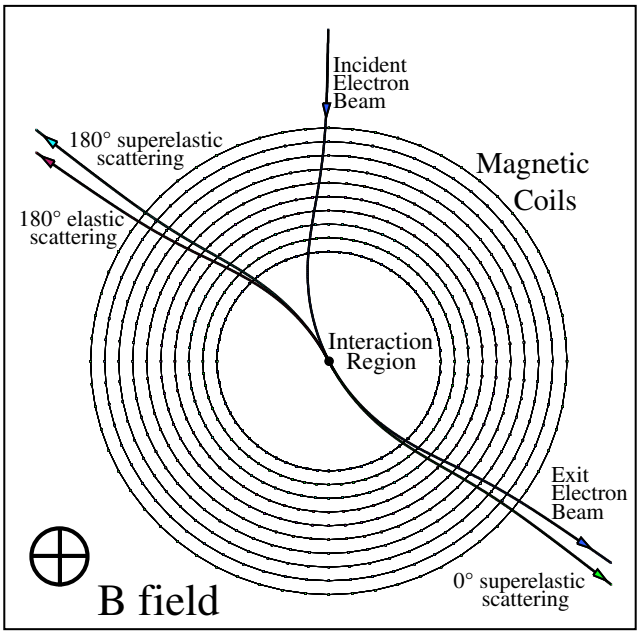

FIG. 2 (color online). Electron trajectories due to the MAC field for an incident energy of 45 eV and a B field at the interaction region of 2.5 mT. The incident electron beam passes through the interaction region and exits at an angle ~55°. Electrons scattered from the interaction region are then steered to angles where an electron energy analyzer can be located. The full scattering geometry from $\theta_e = 0°$ to $\theta_e = 180°$ can therefore be accessed for the first time.

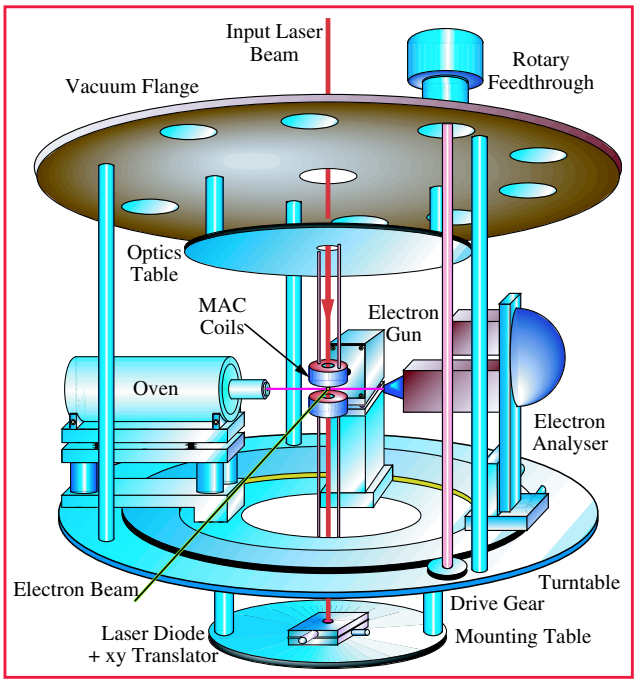

FIG. 3 (color online). The superelastic spectrometer. Atoms emitted from the oven are laser excited by the input laser beam which follows a tracer beam from the laser diode inside the vacuum chamber. The electron gun is located next to the oven, and the analyzer rotates on a turntable driven by a rotary feedthrough. The MAC coils surround the interaction region as shown.

The polarization of the exciting laser is controlled from outside the vacuum chamber.

One consequence of using the MAC device is that the excited substates of the target atom are no longer degenerate. For the superelastic scattering studies presented here, calcium was excited to the 4^1P_1 state by circularly polarized laser radiation at ~423 nm. This means that the quantization axis of the laser radiation is parallel to the magnetic field generated by the MAC, and so the laser-excited states are as shown in Fig. 4. The magnetic field removes the degeneracy of the $|L, m_L\rangle = |1, \pm 1\rangle$ substates which are coupled to the ground state by circularly polarized radiation as shown. To measure $L_\perp$ it is therefore necessary to retune the laser frequency for each selected polarization state by twice the Zeeman shift, so as to remain in resonance throughout measurements. $L_\perp$ is then determined from the superelastic signal $S_{\mathrm{Polzn}}(\theta_e)$ using the expression

$$L_\perp = \kappa \frac{S_{\mathrm{LHC}}(\theta_e) - S_{\mathrm{RHC}}(\theta_e)}{S_{\mathrm{LHC}}(\theta_e) + S_{\mathrm{RHC}}(\theta_e)}, \qquad (1)$$

where κ is an optical pumping term which depends on the laser coupling of the ground and excited substates [3]. In the case of calcium, $\kappa = 1$.

Determination of γ and P_{lin} is more involved than for $L_\perp$, since the laser beam is linearly polarized for these measurements, and so the natural quantization axis of the laser (along the laser polarization axis) and the **B** field from the MAC are orthogonal. A common axis must be defined, and it is sensible to again choose this along the **B** field. In this case the laser polarization is represented as a superposition of RH and LH circularly polarized radiation, and the interaction is considerably more complex. A full description of the techniques required to determine γ and P_{lin} from the data will be presented in a future paper [7].

The experiment using the MAC device was conducted for outgoing electron energies $E_{\mathrm{out}}^{\mathrm{super}} = E_{\mathrm{inc}}^{\mathrm{coinc}} = 45$ eV, 55 eV. The electron energy from the gun was set 2.93 eV lower than these energies, with a beam current of 5 μA.

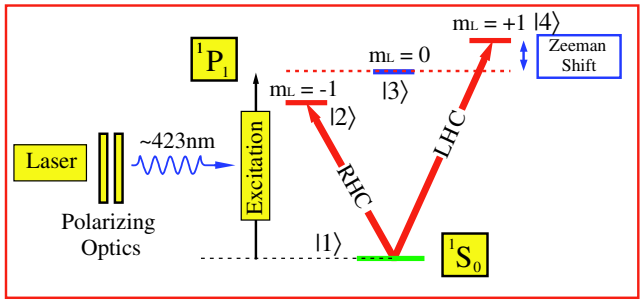

FIG. 4 (color online). Laser excitation of calcium to the 4^1P_1 state at ~423 nm using circularly polarized radiation. The $m_L = \pm 1$ excited substates are shifted in energy due to the magnetic field, and so the laser frequency must be altered to ensure atoms remain in resonance when the laser polarization is adjusted to perform $L_\perp$ measurements.

The calcium oven was operated at a constant temperature of 1060 K. The laser intensity at the interaction region was ~40 mW/mm^2, and the rates of superelastically scattered electrons varied from ~10 Hz to ~3 kHz, depending on the selected scattering angle. The vacuum chamber pressure was $\sim 1 \times 10^{-6}$ torr for all measurements.

Figure 5 shows the results of the experiments, where the $L_\perp$ parameter is derived as in Eq. (1). At 45 eV, the new results are compared to the superelastic scattering data of Law and Teubner [8], who measured $L_\perp$ for scattering angles $\theta_e \sim 0°$ to $\theta_e = 90°$. The early electron-photon coincidence measurements of Kleinpoppen and co-workers [9] from $\theta_e = 10°$ to $\theta_e = 50°$ are also shown for comparison. It is clear that the quality of the present

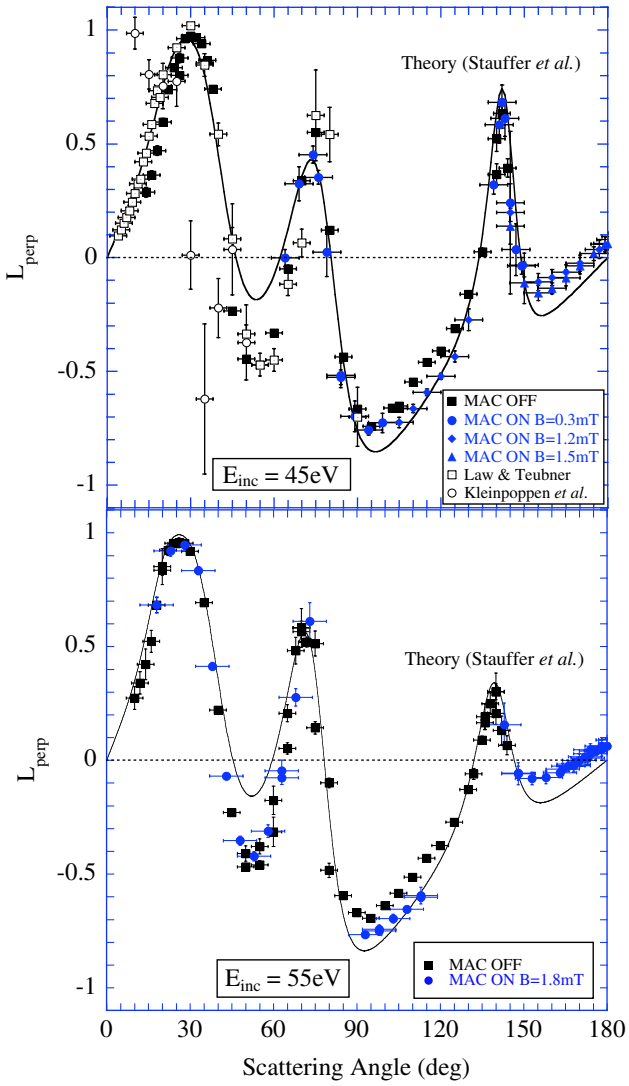

FIG. 5 (color online). Derived values of the angular momentum parameter $L_\perp$ from experimental data for outgoing electron energies 45 and 55 eV, at angles from $\theta_e = 0°$ to $\theta_e = 180°$. The results at 45 eV are compared to the superelastic data of Law and Teubner [8] and to the coincidence data from Kleinpoppen and co-workers [9]. The theoretical calculations of Stauffer and colleagues [11] are also shown. For details, see text.

measurements is much greater than those of the coincidence measurements, which have difficulties with low counting rates and long data accumulation times.

The new results presented here include measurements from $\theta_e = 14°$ to $\theta_e = 145°$ taken without the MAC operating, and data up to (and beyond, not shown) $\theta_e = 180°$ taken with the MAC operating with different **B** fields. The results with and without the MAC operating are in close agreement where overlap exists, differences being due to small changes in the contact potentials around the interaction region which occurs due to calcium deposition [10].

Data were taken using a range of **B** fields at this energy since it was found that the MAC produced significant amounts of noise on the signal at certain angles, making data collection in these regions difficult. This noise is thought to emanate from electrons scattered from the walls of the vacuum chamber which reenter the MAC and are then steered into the analyzer. This effect has been seen before, and can be resolved by changing the solenoid field to steer the unwanted electrons away from the analyzer.

The results at 55 eV are again shown from $\theta_e = 14°$ to $\theta_e = 145°$ taken without the MAC operating, and for selected angles from $\theta_e = 14°$ to $\theta_e = 180°$ with the MAC operating. A larger **B** field equal to 1.8 mT was chosen since the electron energy is higher than for the measurements at 45 eV. In this case, only one set of data was needed with the MAC operating. No other experiments have been conducted at this energy for comparison.

The calculations of Stauffer and colleagues [11], convoluted with the experimental angular response, are also shown for comparison. It is clear that this model is in very good agreement with all superelastic data that have been taken, apart from the minimum at $\theta_e \approx 60°$ which is underestimated at both energies, and the minima at the higher energies that are overestimated. The maxima and their positions are reproduced well. In particular, the sharp peak at $\theta_e \approx 150°$ which is observed for the first time in the present measurement, is in very good agreement with theory. It is clear that the theoretical model has described the physics of the collision for the $L_\perp$ parameter well at these energies.

It is of interest to note that experimental results for elastic scattering from inert gas targets which also use a MAC device [12] show significant discrepancies with other calculations by Stauffer and colleagues [13], who use a similar theory to calculate elastic cross sections for these targets. Since the theoretical derivation of the natural frame parameters is considerably more involved than for elastic cross sections, it is noteworthy that such excellent agreement is found here compared to that for elastic scattering, since both experiments employ a MAC device. The new results presented here tend to confirm that previous elastic scattering data taken in the region beyond that which can be accessed conventionally are therefore reliable. The discrepancy between theory and experiment for elastic scattering from noble gas targets may therefore be due to the increased importance of polarization effects at low incident energies, rather than being due to a systematic problem in the experiment.

It is finally worth noting that this program of work has direct application in many other fields which use laser and magnetic fields to interact with atoms and molecules. Most noteworthy is that of atom manipulation, which employs magnetic and laser fields to cool and trap atoms. The models developed here can be directly applied in this research area, with the advantage that the full dynamics of the interaction can be modeled accurately. These techniques are already being applied to atom traps in the authors' laboratory, and it is fully expected that others in the field will also make use of the general techniques developed here.

The authors would like to thank the EPSRC, U.K. for providing funding for this project, and would also like to thank Alan Venables, Dave Coleman, and Dr. Nick Bowring for providing technical and computational support.

[1] N. Andersen, J. W. Gallagher, and I. V. Hertel, Phys. Rep. **165**, 1 (1988).
[2] I. E. McCarthy and E. Weigold, *Electron Atom Collisions* (Cambridge University Press, Cambridge, U.K., 1995), Vol. 1, p. 1.
[3] P. Farrell, W. R. MacGillivray, and M. C. Standage, Phys. Rev. A **37**, 4240 (1988).
[4] F. H. Read and J. M. Channing, Rev. Sci. Instrum. **67**, 2372 (1996).
[5] A. J. Murray, M. J. Hussey, and M. Needham, Meas. Sci. Technol. **17**, 3094 (2006).
[6] M. J. Hussey and A. J. Murray, Meas. Sci. Technol. (to be published).
[7] M. J. Hussey, A. J. Murray, W. R. MacGillivray, and G. C. King, Phys. Rev. A (to be published).
[8] M. R. Law and P. J. O. Teubner, J. Phys. B **28**, 2257 (1995).
[9] M. A. K. El-Fayoumi, H. Hamdy, H.-J. Beyer, Y. Eid, F. Shahin, and H. Kleinpoppen, At. Phys. **11**, 173 (1988).
[10] A. J. Murray and D. Cvejanovic, J. Phys. B **36**, 4875 (2003).
[11] R. K. Chauhan, R. Srivastava, and A. D. Stauffer, J. Phys. B **38**, 2385 (2005).
[12] B. Mielewska, I. Linert, G. C. King, and M. Zubek, Phys. Rev. A **69**, 062716 (2004).
[13] R. P. McEachran and A. D. Stauffer, J. Phys. B **16**, 4023 (1983).